Energy & Buildings 363 (2026) 117564

Contents lists available at ScienceDirect

Energy & Buildings

journal homepage: www.elsevier.com/locate/enbuild

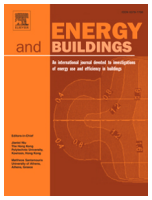

A probabilistic assessment of hail hazard impact on the life cycle of BMPV systems

Rocco di Filippo *, Gianluca Maracchini, Rosa Di Maggio, Oreste S. Bursi, Rossano Albatici

Depart. of Civil, Env. & Mechanical Engineering, University of Trento, Via Mesiano 77, Trento, 38123, Italy

A R T I C L E I N F O

Keywords:
Hail risk
BMPV
EROI
Buildings
Lifecycle
PV

A B S T R A C T

Building-mounted photovoltaics (BMPV) are increasingly used for sustainable and autonomous energy generation in the built environment. Furthermore, policies are pushing BMPVs as enablers of a decarbonized energy grid. Their lifecycle performance is a critical factor influenced by environmental hazards. Among others, hail hazard poses a significant threat. This study presents a probabilistic risk assessment of hail hazard for BMPV systems. By leveraging the performance-based engineering approach, it incorporates hail hazard, physical vulnerabilities, and consequence modelling. The analysis employs hazard models to predict hail frequency and specific intensity measures linked to damage scenarios for BMPV. Hail size is found to be well correlated with expected damage to the front glass, making it a viable intensity measure. Hail risk can reduce the operational lifespan of BMPV by up to 10.87 years and the Energy Return on Energy Invested (EROI) by 46.52% when the glass thickness is 3.2 mm, and 2.22 years and 15.07% for a 4 mm thickness. Repair costs are significant compared to both the BMPV initial costs and the hail-related expected losses of whole buildings. This study underscores the importance of hail risk assessment for BMPV lifecycle analyses and of setting minimum impact resistance based on hail hazard levels.

1. Introduction

The building sector accounted for approximately one-third of global energy consumption in 2019 [1]. To decrease reliance on fossil fuels, reduce the carbon footprint of buildings, and enhance their overall energy efficiency, numerous building regulations have been implemented over the last thirty years [2,3]. A large share of building energy consumption is devoted to heating and cooling [4]. The necessary thermal energy can be produced by technological systems, such as heat pumps, that run on electricity. In this respect, building-mounted photovoltaics (BMPV) can provide electricity to support buildings' energy needs [5,6]. As a result, the importance of BMPV as an energy source cannot be underestimated, especially considering the current decarbonization efforts [6,7]. The analysis of BMPV lifecycle performances carries, therefore, a significant role. Studies have focused on the assessment of such performances for PV technology, differentiating between ideal conditions and empirical data [8,9]. In particular, it appears that the actual lifetime of PV equipment may be in some cases shorter than expected [10]. There are numerous mechanisms of performance degradation [11]. These mechanisms can often be the combination of failures from system components [12], external forces [13] and environmental factors [14]. Concerning the latter, climate change effects have been linked to reliability and performance risks for PV technology [14]. Among the possible detrimental interactions, a notable one is related to natural hazards and their external actions [11,14]. Indeed, climate change has been linked to an increased likelihood of weather-related disasters such as floods [15], hurricanes [16] and wildfires [17]. Hence, the issue of PV climate resilience cannot be neglected [18]. Along this line, methods for probabilistic risk assessment have already been applied to predict extreme winds impact on BMPV systems [19,20]. Another source of potential damage for BMPV is hailstorms, as documented by empirical [21–24] and experimental data [25]. Besides, whilst international standards prescribe a certain resistance to hail impact, this produces different levels of actual reliability [26,27]. For instance, the IEC 61,215 [28] prescribes a hail size for testing of 25 mm, which is not enough in case of hail-prone areas [24]. While manufacturers may adopt more severe testing guidelines, as per the non-mandatory IEC 63,397 [29], the issue of assessing the hail reliability of PV panels remains. The hail risk research has focused on hazard models [30] and consequence analysis [31,32]. Several building components have been found vulnerable to hail [33], including windows [34], ETICS [35,36], cladding systems [37], roofs [38,39]. Concerning the latter, performance-based engineering (PBE) methods for risk assessment have been applied to evaluate expected annual losses (EAL) taking into account both hazard and damage models [37–39]. Indeed, the risks linked to natural hazards are often assessed using PBE methods [40] that, based on the total probability theorem, allows for

* Corresponding author.
E-mail address: rocco.difilippo@unitn.it (R. di Filippo).

https://doi.org/10.1016/j.enbuild.2026.117564
Received 2 October 2025; Received in revised form 9 April 2026; Accepted 29 April 2026
Available online 5 May 2026

Abbreviation	Definition
BMPV	Building-mounted photovoltaics
DM	Damage Measure
DV	Damage Variable
EDP	Engineering Demand Parameter
EROI	Energy Return on Energy Invested
IM	Intensity Measure
AB	Apartment block
PBE	Performance based engineering
SFH	Single-family house
Notation	**Definition and Units**
C_{pv}, C_b	Annual GHG emissions of BMPV and buildings ($kgCO_{2eq}/(m^2 \cdot y)$)
Cr	GHG emission ratio
$\Delta EROI$	EROI reduction
ΔLf	Lf reduction
Dh	maximum hailstone size (mm)
D_d	hailstone size for damage (mm)
D_r	hailstone size resistance (mm)
FCC	Fraction of construction cost
Fd, Fb	BMPV and buildings fragility functions
EAL	Expected annual loss (%)
Fh	Expected hailstorms days (y^{-1})
EC_{pv}, EC_b	Embodied carbon of BMPV and buildings (€/m^2)
LEHA	Largest expected hail size on a reference area (mm)
Lf	Service life of a BMPV system (years)
MDR	Mean Damage Ratio
MESHS	Maximum expected severe hailstone size (mm)
M_{pv},M_b	Annual monetary costs of BMPV and buildings (€/($m^2 \cdot y$))
Mr	Monetary costs ratio
P_{hf}	Annual probability of failure
Tg	PV front glass thickness (mm)
UC_{pv},UC_b	Unit cost of BMPV and buildings (€/m^2)
ζ	Probability of failure over Lf

an independent evaluation of hazard, fragility, damage, and loss. PBE has been adapted and applied to different hazards, such as tsunamis [41], hurricanes [42], wind [43], floods [44], coastal hazards in general [45] and fires [46,47]. Furthermore, PBE has also been applied to evaluate the environmental impacts of natural hazards-induced damages to technological components [48,49]. These impacts are mainly relevant to the embodied carbon of repair activities [50] and, in some cases, to the emission of polluting compounds [43]. The peculiarity of BMPV systems implies that, in case of damage, environmental impact may derive from embodied carbon due to repair or replacement [51,52] or missed low-GHG energy production [19,24]. The energy output over the lifecycle of BMPVs is of critical importance and, whilst they are a key tool to prevent climate change, hail hazard may diminish their efficacy and increase the likelihood of an "energy-emission" trap [53]. In fact, according to [53], the energy necessary to decarbonise the energy grid itself could impact the remaining emission budget. In this respect, the energy return on energy investment (EROI, also called ERoEI) is an important measure for performances of PV applications [54–56]. Still, there are no studies on probabilistic hail risk assessment for BMPV systems to date. To fill this gap, this paper has the following research goals, also corresponding to the phases of this study:

1) Present a feasible quantitative methodology to define the hazard, vulnerability and consequence components of PBE in Section 2.
2) Develop an analytical response model for PV panels under hail action with respect to front glass breakage.
3) Provide a numerical application to a BMPV case study placed in three geographical locations (Switzerland, The Netherlands and Canada) according to three consequence metrics (monetary cost, environmental impact and energy cost). Assessing, on these bases, whether the hail risk is significant, also considering the reduction of service life.
4) Compare hail risk for BMPV systems to whole buildings. Determine if the BMPV systems represent a non-negligible share of hail risk for buildings.

Hence, the research questions that will be answered are: i) can a PBE approach be effectively adopted for hail risk assessment for both BMPVs and buildings?, ii) Is the expected impact for BIPVs significant?, iii) Is the expected impact for BIPVs significant when compared to that of the whole building? The results are then discussed in Section 4, whilst the main conclusions of the study are drawn in Section 5 along with some comments on future developments.

2. Methodology

The foundational methodology hereby adopted for hail risk assessment is PBE. The analytical formulation of the PBE framework is given by:

$$\lambda(DV) = \int\int\int P(DV|DM)dP(DM|EDP)dP(EDP|IM)d\lambda(IM) \quad (1)$$

where $\lambda(IM)$ represents the hail hazard, quantified as the rate at which the hail action exceeds a specified intensity measure (IM). The term $dP(EDP|IM)$ represents the probability that the system will experience a given response, quantified in an Engineering Demand Parameter, EDP, conditioned on the intensity measure IM, and is typically expressed as a fragility curve [57]. The term $dP(DM|EDP)$ denotes the probability that a given EDP results in a damage state DM. Additionally, $P(DV|DM)$ represents the conditional probability of a specific decision variable or consequence measure (DV), typically related to fatalities or economic costs, given the DM. Finally, $\lambda(DV)$ indicates the rate at which the consequence measure exceeds a specified threshold, which defines the expected impact of the hail hazard on the system under study [58–60]. The application of the PBE entails several assumptions, among them i) any damaged system is repaired or replaced, ii) the repaired or replaced system is the same as the original one. The hazard, response and consequence models are presented in Sections 2.1–2.3 respectively.

2.1. Hazard model definition

In this Section we will define hail hazard models for three geographical locations i.e. Switzerland, The Netherlands and Canada. The hazard level, i.e. $\lambda(IM)$, for hail should represent a rate of exceeding a meaningful IM. The selection of IM is not straightforward given that the damages depend on the complex impact dynamic. Multiple parameters can influence the impact effects, such as hail size [32,38,39], attack angle [38], kinetic energy [61], impulse rate [27,62] and momentum [25]. In this work, we will focus on hail size, which is the most used IM in both hazard and response models. Hail size is commonly equated to the diameter of an ideally spherical hailstone and the relevant IM would be the maximum hailstone diameter expected, Dh. Country-based hail hazard models, such as for the Netherlands [63] and Switzerland [64], provide the return time, T_r, for a given Dh. This allows the evaluation of the yearly probability of exceedance of a given Dh, which can constitute the hazard function $\lambda(IM)$ with $IM = Dh$.

Usually, these models adopt a given area of 1 km^2 [63,64]. Hence, when analysing systems with a different area, A_s, the values of Dh should be scaled. In this respect, [64,65] differentiate between "*Maximum expected severe hail size*", MESHS, and "*Largest expected hail size on a reference area*", LEHA. Although MESHS is referred to an area of 1

km^2, an analytical formulation allows a conversion to a reference area as follows:

$$LEHA(A_s) = MESHS + 0.0919 \cdot log_{10}(A_s) \cdot MESHS + 0.00834 \cdot log_{10}(A_s) \quad (2)$$

where LEHA and MESHS are expressed in mm^2 and A_s in km^2. This relationship has been calibrated for the Swiss hazard models but, in this work, we will also consider it valid for the other hazard models considered. This choice introduces a source of uncertainty, which, lacking higher-resolution hail hazard data, is difficult to quantify. However, the trend of size reduction between LEHA and MESHS, when smaller areas are considered, is intrinsically valid for any geographies. Values from [63] are relevant to an area of $1km^2$.

Another way to build the hazard function is to start from less aggregated data as shown by [38] in a hail risk assessment for a Canada region. The first element to consider is the hailstorm frequency, Fh, i.e. the expected hailstorm days in a year [66]. Then, conditioned to the occurrence of a hailstorm, it is possible to use an empirical formulation to describe the probability distribution of Dh. Leveraging the analysis of a database of 37,000 observations from North America from [38,61] defined the following relationship:

$$CDF_{Dh}(Dh) = 1 - \frac{e^{(m \cdot Dh + b)}}{e^b} \quad (3)$$

where m and b are empirical values equal to $0.111\,\text{mm}^{-1}$ and 6.55 mm respectively. Eq. (3) does not discriminate in the area considered. Still, the empirical values refer to records from hailpads with an area in the order of a square meter. The yearly probability of having a hailstorm exceeding a certain Dh can be obtained by combining Fh with CDF_{Dh} from Eq. (3) as follows:

$$P(X > Dh) = Fh \cdot CDF_{Dh} = 1/T_r(Dh) = \lambda(Dh) \quad (4)$$

We will assume $A_s = 2m^2$, a widespread dimension for an independent PV panel, for the Switzerland and Netherlands models and a $Fh = 0.5y^{-1}$ for the Canada model. According to [66], this corresponds to a predominant share of the Canadian territory. It is useful to note that in some areas Fh can reach 4 hail days per year. Since Montreal falls in this area, it will be selected as the reference for the Canadian hail hazard model. For the Swiss one, we will refer to the Bern area. For the Netherlands, [63] reports the curves for the 4 NUTS-1 regions and we selected the Noord region, whose largest city is Groningen. For Bern and Groningen areas, the available data cover up to a return time of 100 years, i.e. an annual frequency of 10^{-2}. However, the linear trend in the semilogarithmic space has been prolonged up to an annual frequency of 10^{-2}. The resulting $\lambda(Dh)$ functions from Eq. (4) are depicted in Fig. 1.

From Fig. 1, it is possible to appreciate that MESHS curves are more severe than those referred to A_s. This was expected given that they refer to a larger area. Moreover, Montreal and Bern curves exhibit the highest and lowest maximum diameters, respectively.

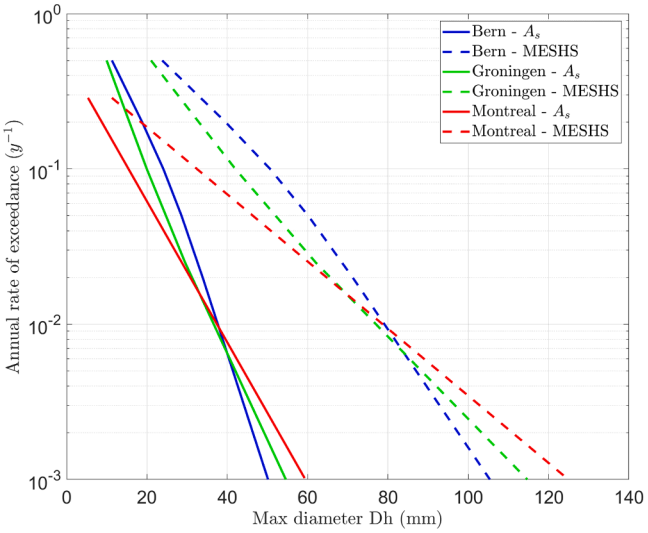

Fig. 1. Hail hazard curves for Bern, Groningen and Montreal relevant to MESHS and A_s.

Fig. 2. BMPV systems damaged by the July 2023 hailstorms in Italy [68]. Photo of Leonardo Secchi from [69].

2.2. Response models

A response model usually describes the relationship between the external action and the behavior of the system under study [67]. It is also used in PBE-based methods to predict damages based on the IM of a given natural hazard. In this subsection, we will present the methodology to analytically define a response model for PV panels in Section 2.2.1 and for buildings in Section 2.2.2. Notably, given that the hazard models defined in Section 2.1 use Dh as IM, our models should adopt the same IM.

2.2.1. PV panels

Due to hail impact, PV panels can undergo visible damage, such as breakage of the front glass and invisible ones [14,23]. In this work, we will consider only the breakage of the front glass, which can produce a partial to complete loss of solar cell functionality [14,23]. We define such a damage state as DS_g. See for reference Fig. 2.

The response model should define the probability of DS_g as a function of Dh. This probability is set to follow a cumulative distribution function, defined as $Fd(Dh)$, that can be analytically expressed as:

$$Fd(Dh) = P(DS_g|Dh) = \phi\left[\frac{ln(Dh/m_d)}{\beta_d}\right] \quad (5)$$

where ϕ indicates a lognormal cumulative distribution function, which is rather common in the definition of fragility functions [20]. Besides, m_d and β_d are the median and the dispersion of the distribution.

To define $Fd(Dh)$, the necessary data can be retrieved from different sources. The first is to refer to the international standards that set minimum hailstone diameter resistance, defined as D_r, such as the IEC 61,215 [28] or other national codes [27]. On this basis, one may assume that the probability with D_r of DS_g, able to put the system out of service, would be reasonably low. However, this can only provide a lower bound for the damage model, without any information on the actual damages for diameters higher than D_r.

In this respect, the second approach relies on empirical or testing data, which can be either from real hailstorm damage statistics [22,24] or experimental test campaigns [25]. The limitation with the damage

Table 1
D_r and D_d for PV panels with different Tgs.

Tg (mm)	D_r (mm)	D_d (mm)
2.8	35	45
3.2	35	45
4	55	//

statistics of [22] is that they are related to insurance claims, and not all damages are either covered or claimed. Jordan et al. [24] instead focuses on the loss of performance of systems after hailstorms. The relationship between hail size, not measured precisely, and damage is not proportional, as other factors, such as wind, may influence it during a hailstorm. Furthermore, for both [22] and [24], many characteristics of PV systems under study are not available. As a result, purely empirical are too incomplete to be used as a primary source.

Hence we will rely on the experimental data from [25] which allows us to define a threshold for both D_r and the hailstone diameter corresponding to DS_g, defined as D_d. In detail, the tests involved four diameters, i.e. 25, 35, 45 and 55 mm with proportionally higher terminal velocity. The terminal velocities were roughly between 25 m/s for the 25 mm diameter and 35 m/s for the 55 mm diameter, which aligns with several available models [70]. The study also considers three thicknesses of the front glass, Tg, i.e. 2.8, 3.2 and 4 mm, from commercially viable PVs. Ten rounds for each diameter are performed from the smallest to the largest and the procedure is stopped after breakage of the glass. On such a basis, we can set D_r equal to the biggest diameter that caused no breakage and D_d to the first that broke the glass. The results are reported in Table 1.

As reported in Table 1, D_r is larger than 25 mm for each Tg, which is expected since IEC 61,215 prescribes a specific diameter for PV testing according to the MQT 17 protocol [28]. For instance, the US FEMA recommends a minimum Tg equal to 3.2 mm [71]. Data for 4 mm Tg lacks a D_d since, even for a 55 mm hailstone diameter, the glass did not break. Still, other damage metrics were recorded, such as the negative variation in peak power generation, which showed a certain reduction, albeit relatively small. Hence, it is reasonable to think that a diameter than 55 mm may indeed break the front glass. Moreover, no experimental data are available in the interval between D_r and D_d for smaller Tg. To fill these gaps and build the fragility function $Fd(Dh)$, the following assumptions are adopted:

i) The damage, i.e. DM from Eq. (1), will be considered conditioned exclusively by the selected IM, i.e Dh, without considering the influence of any intermediate EDP. Thus, in Eq. (1), the role of any EDP between DM and the IM is neglected.
ii) Only one damage state will be considered, implying a major failure of the front glass: "glass breakage damage state" or DS_g.
iii) The probability of DS_g conditioned to D_r is set to be reasonably low, i.e. $P(DS_g|D_r) = 0.05$. This is somehow justified by the fact that in the tests, each Tg underwent 10 different hits from D_r hailstones.
iv) The probability of DS_g conditioned to D_d is set equal to 0.95, i.e. $P(DS_g|D_s) = 0.95$. Indeed, in the tests, a single D_d hailstone was enough to break the 2.8 and 3.2 mm glasses.

Given that 2.8 and 3.2 mm Tg share the same D_r and D_d, the resulting $Fd(Dh)$ will be equivalent and defined as Fd_{p1}. For the 4.0 mm Tg, we cannot adopt assumption iv) since the glass did not break and there is no D_d. Hence, the resulting $Fd(Dh)$, i.e. Fd_{p2}, is derived by adopting the same β_d of Fd_{p1} and deriving m_d with the additional condition of assumption iii).

The effect of damage accumulation is considered already included in the probabilistic fragility functions. This is because, differently from other components [37,38,72], there are not enough data to better describe this phenomenon for PV systems. The influence of angles of incidence lower than 90 degrees, i.e. the inclinations used in the experimental tests of [25], is not considered. This is consistent with the approach of [38,39] adopted for roofs and builds on the empirical evidence that incidence angles higher than 45 degrees do not affect much the energy of hailstones hits. The sensitivity of the risk analysis to the assumptions i)-iv) is expected to be high. However, the analytical model can be updated in case more experimental data would be available. For simplicity, we define the panels type P_1, with Tg up to 3.2 mm, and P_2 with Tg of 4 mm.

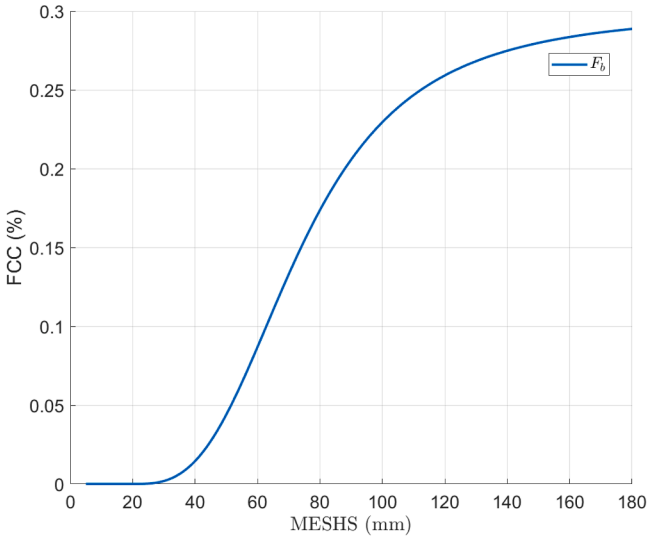

Fig. 3. Fragility curve F_b - FCC as a function of MESHS.

2.2.2. Buildings

The definition of a damage model for buildings is needed to fulfill the research goal 3) as presented in Section 1. There are not many quantitative damage models for building damage due to hail hazard, with [32,73] among these. In detail, [32] analyzed a database of $2.5 \cdot 10^5$ insurance claims relevant to hail damage in Switzerland over 20 years. The considered damage metric is the ratio between damage cost and the monetary value of the insured asset, i.e. mean damage ratio or MDR. We will, however, convert this metric into a ratio between the repair or damage costs and the construction costs. This approach is often used in risk assessment [6,74,75] to compute the expected annual loss, EAL, and allows for a direct comparison between areas that may have different market values. Moreover, MDR is influenced by both land and market values, thus rendering any assessment time-specific. Hence, to shift from MDR to a fraction of the construction cost, FCC, as a damage metric, it is necessary to quantify the ratio between the market value and the construction cost. According to industrial sources, the building cost per square meter in Switzerland is roughly 3250 CHF/m^2 [76] whilst the market value is 8255 CHF/m^2 [77]. Hence, we can write the ratio between MDR from [32] and FCC is 2.54.

In [32], the authors derive the parameters of a sigmoidal function to fit the statistical data and correlate MDR with MESHS. The analytical definition of the curve is derived from [78]. The adaptation of the curve from MDR to FCC is depicted in Fig. 3.

The curve depicted in Fig. 3 adopts MESHS as IM even if the area of a building is, most often, less than 1 km^2. However, this effect is already accounted for, given that the curve is derived from empirical data.

It should be noted that a similar research has been carried out on data from 2010 to 2020 related to 30 hail events in Australia [73]. We have, however, not considered it because the damage metric was damage costs on the maximum insured value, thus excluding the value of the insured asset.

2.3. Consequence metrics

In this section, we define the consequence metrics for BMPV systems and buildings in terms of monetary losses and carbon emissions.

2.4. BMPV metrics

For BMPV systems, any damage from hail can result in three types of measurable consequences:

(a) Monetary costs, due to the replacement or repair of the damaged system;
(b) Embodied carbon emissions, linked to the use of materials in the activity of repair or replacement of the system;
(c) Energy costs, associated with the period needed for the repair or replacement of the system and the related loss of energy production for any downtime.

To estimate (a), it is useful to recall that the damage state considered in Section 2.2.1 corresponds to a severe front glass breakage. This damage would make the system unusable, requiring a replacement. We can hence approximate the corresponding costs to 100% of the system cost. The system cost has to be assessed considering that, in Section 2.1, we set $A_s = 2m^2$. However, to facilitate the following analyses, we define a unit cost of BMPV per square meter of the system, UC_{pv}. As a premise, we will consider P_1 and P_2 to have the same unit cost and embodied carbon, thus assuming the influence of Tg is negligible. Based on [79] we can write $UC_{pv} = 350\ €/m^2$.

To confirm this value with a different source, we compare the case of the Italian market and rely on the same methodology from [6,80]. Considering the widely adopted mono-crystalline silicon technology, this system would entail a peak power of roughly 300 W. Thus, from the official price list for tenders and contracts, we derive a max allowed cost of 2400 €/kWp. Hence, the system considered will cost 800 €and we can derive a unit cost of 400 $€/m^2$. The figure aligns with the UC_{pv} defined above, given that this value i) is a maximum, ii) comprises any support structure.

From an analytical viewpoint, the relationship between the consequence and the damage, described by the probabilistic term $P(DV|DM)$ in Eq. (1), is instead assumed as deterministic. Hence, the parameter M_{pv} is defined as the expected annual monetary losses from hail hazard, and can be calculated by rewriting Eq. (1) as follows:

$$M_{pv} = \lambda(DV) = UC_{pv} \cdot \int_0^{Dmax} Fd(Dh)d\lambda(Dh) = UC_{pv} \cdot P_{hf}(Fd) \tag{6}$$

where Dmax = 120 mm, assuming any higher Dh will have no further impact on any $\lambda(DV)$, given the associated low probabilities. P_{hf} is the resulting annual probability of failure due to hail risk.

Concerning the metric (b), the embodied carbon of PV systems can be defined as a quantity of CO_{2eq} per kWh of energy produced [51,81,82], kWp capacity [83] or square meter [52]. To be consistent with the analysis, we define EC_{pv} as the GHG emissions from embodied carbon equivalent linked to the production of a square meter of PV system. From [52] an average value of roughly 160 $kgCO_{2eq}/m^2$ for polycrystalline technology, can be derived accounting only for front glass and cells produced in Europe. Hence, the annual expected GHG emissions due to hail damage, C_{pv}, can be written as follows:

$$C_{pv} = EC_{pv} \cdot P_{hf}(Fd) \tag{7}$$

C_{pv} should not be confused with the annual amortisation of the embodied carbon, which depends on the finite lifetime of any PV system, i.e. L_f. In fact, C_{pv} is an additional contribution due to the damage-induced reduction of Lf, which we define here as ΔL_f.

Metric (c) can be considered to be two separate terms. Starting from the energy cost for replacement, this is strongly correlated to C_{pv} and can be in the range of 2–3000 MJ per square meter of PV with polycrystalline technology. In addition, the system downtime, Td, will also result in missed energy production. To better appreciate the combination of these two contributions, we will quantify the impact on the EROI parameter, $\Delta EROI_h$. The EROI is defined as the ratio between the energy produced by the system and the energy invested in the system [56]. We define $\Delta EROI_h$ as follows:

$$\Delta EROI_h = \frac{EROI_s - EROI_h}{EROI_s} \tag{8}$$

where $EROI_s$ and $EROI_h$ are the EROI without and with accounting for hail damage, respectively. Considering Ep and Ei the energy produced and invested, $EROI_s = \frac{Ep}{Ei}$, while $EROI_h$ can be written as follows:

$$EROI_h = \frac{Ep \cdot (1 - \frac{Td \cdot \zeta}{Lf})}{Ei \cdot (1 + \zeta)} \tag{9}$$

The parameter ζ is the lifetime probability of failure, which, according to a Poissonian model of hail hazard [38], can be calculated as follows:

$$\zeta = 1 - (1 - P_{hf}(Fd))^{Lf} \tag{10}$$

where Lf is set equal to 25 years as in [55,56,84]. Notably, we assume the failure to be equivalent to a system replacement. Hence ζ represents the failure of the first system, not the cumulative probability of having multiple failures of consequently replaced systems. Although there is no available data about Td, assuming the involvement of an insurance [22] it is reasonable to assume that the process may be longer than the time materially required for a BMPV replacement. Still, the actual loss in energy production would depend on the specific month of the year and the site-specific solar radiation [85,86]. However, even assuming Td equal to 1-2 months, the term $\frac{Td}{Lf}$ is in the order of 10^{-2} and thus negligible. Hence, after some manipulations, Eqs. (8) and (9) can be combined to obtain:

$$\Delta EROI_h = \frac{\zeta}{1 + \zeta} \tag{11}$$

Eq. (11) does not include $EROI$ variations deriving from degradation due to lower hail damage levels, significantly delayed repair, and the possible interaction with other degradation causes. In these cases, the negative effects may even be higher.

In addition to the three metrics above, we can evaluate the resulting loss of service life years, ΔLf_h. It is assumed that: i) for a probability equal to (1-ζ) the system undergoes no reduction of Lf, ii) for a probability equal to ζ, the failure due to hail can happen in any moment of Lf, hence with an average of $\Delta Lf_h = Lf/2$. Thus ΔLf_h can be calculated as follows:

$$\Delta Lf_h = Lf - (1 - \zeta) \cdot Lf - \zeta \cdot \frac{Lf}{2} = \zeta \cdot \frac{Lf}{2} \tag{12}$$

2.5. Buildings metrics

For buildings, we will only consider the expected annual monetary costs, M_b, and embodied carbon emissions, C_b, as risk metrics. An informed estimate of the unitary cost can be derived from [87], which reports cost statistics from several European cities. The average construction cost is roughly 2000 $€/m^2$, which will be the value of UC_b. Therefore, M_b can be calculated as follows:

$$M_b = UC_b \cdot P_{hf}(Fb) \tag{13}$$

The embodied carbon emissions linked to building constructions can be derived from [88]. The report analyses a large dataset of European constructions and defines a harmonized average of roughly 600 $kgCO_{2eq}/m^2$ for residential buildings. This value, set as EC_b, allows the calculation of C_b according to the following:

$$C_b = EC_b \cdot P_{hf}(Fb) \tag{14}$$

To perform a meaningful comparison between buildings and BMPV metrics, the difference in the areas of the two should be considered. This

Table 2
Function parameters of Fd_1 and Fd_2.

Panel type	Function	m_d (mm)	β_d ( )
P_1	Fd_1	39.68	0.076
P_2	Fd_2	62.36	0.076

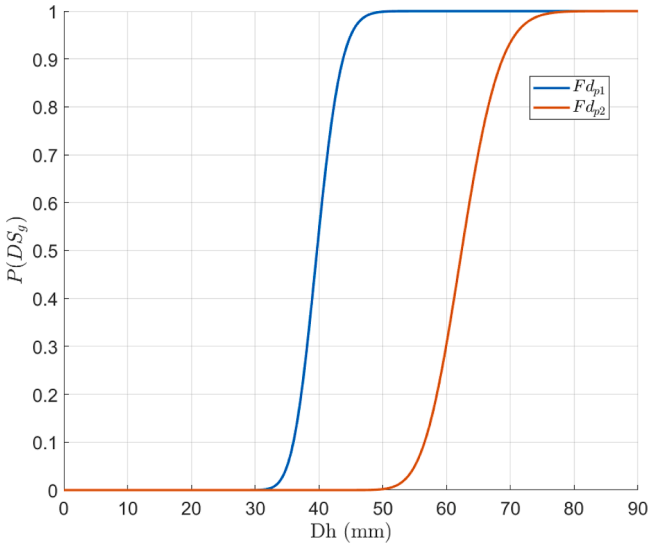

Fig. 4. Fragility curves Fd_{p1} and Fd_{p2}, relevant to Tg of 2.8 and 3.2 mm and 4 mm, respectively.

is because a relatively small BMPV on a rather large building will always result in a negligible share of damage. Although M_b and C_b represent values for square meters, the comparison with PV metrics will be done after adjusting them by a factor, γ, representing the ratio between the building floor area, A_b, and A_s. Hence, we define Mr and Cr as follows:

$$Mr = \frac{M_p}{\gamma \cdot M_b} \quad \text{and} \quad Cr = \frac{C_p}{\gamma \cdot M_b} \tag{15}$$

where the γ values considered in this work will be $\gamma_{SFH} = 10$ and $\gamma_{AB} = 100$. These two values are representative of a single-family house, SFH, and an apartment block, AB, respectively. In practice, these values correspond to a $20m^2$ PV system on a building of $200m^2$ useful floor area for γ_{SFH}, and a $60m^2$ PV system on a building of $6000m^2$ useful floor area for γ_{AB}.

3. Results

The hail response models for BMPVs are expressed in terms of lognormal cumulative distribution functions, i.e. Fd_{p1} and Fd_{p2}. The relevant parameters are listed in Table 2, whilst the functions are depicted in Fig. 4.

The significant difference between Fd_{p1} and Fd_{p2} aligns with other tests on glass resistance [72], which have shown that even a slight increase in thickness can effectively reduce vulnerability. The resulting Fd_{p2}, as depicted in Fig. 4, implies that a 4 mm would certainly break with a Dh close to 80 mm.

Concerning the loss analysis, the expected monetary costs, i.e. M_{pv}, for P_1 and P_2, panels and M_b, are reported in Fig. 5 for each geographical area considered.

Fig. 5 shows that P_1 panels are, by far, the most affected by hail hazard when equal surfaces are considered. Buildings come second in Bern and Groningen but third in Montreal. The different rankings across the locations are the result of the different slopes in both hazard and fragility curves depicted in Figs. 1, 4 and 3. Notably, the expected cost for buildings is in the range of 0.1% of the UC per year. For reference, this EAL is in the same order of magnitude as other natural hazards,

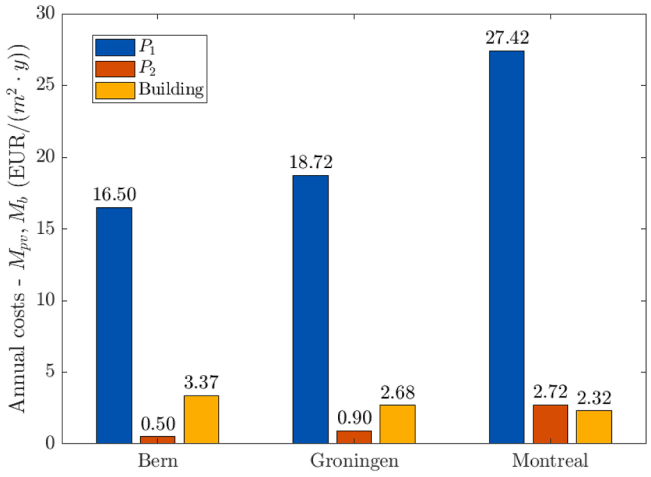

Fig. 5. Expected annual monetary costs due to hail damage for m^2 of panels area for P_1 and P_2, and useful floor area for the building.

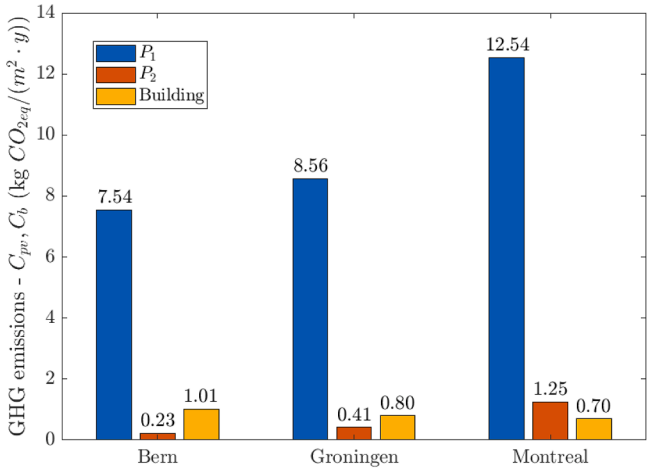

Fig. 6. Expected annual GHG emissions due to hail damage for m^2 of panels area for P_1 and P_2, and useful floor area for the building.

such as earthquakes [74] and floods [6] for Italy. Similarly, the expected GHG emissions, i.e. C_{pv}, for P_1 and P_2, panels and C_b for buildings, are depicted in Fig. 6.

The ranking shown in Fig. 6 is the same as Fig. 5. However, given the smaller difference between EC_p and EC_b compared to UC_p and UC_b, buildings have lower relative emissions when equal surfaces are considered. Overall, the level of emissions from buildings is relatively small next to the operational emissions due to energy consumption, which are, on average, roughly 20–40 times more [6]. However, they became significant when compared to net-zero targets [6]. The resulting losses in service life years, ΔLf_h, for panels P_1 and P_2 are shown in Fig. 7.

The variation of ΔLf_h across the different locations reflects the trend of the other metrics. Overall, ΔLf_h is always above 8.5 years for P_1 panels, whilst for P_2 this reaches almost 10% of the total reference life in the case of Montreal. More in detail, the trend of ζ over Lf is depicted in Fig. 8.

Along the same line, the reduction of the EROI is depicted in Fig. 9. This reduction is between 41 and 46% for P_1 and between 3 and 15% for P_2.

The final comparison of expected monetary costs and emissions, between BIPV and buildings, is reported in Table 3, which lists Mr and Cr values.

It appears that Mr and, to a higher extent, Cr are always significant in the case of an SHF and a P_1 panel, with both being more than 100%

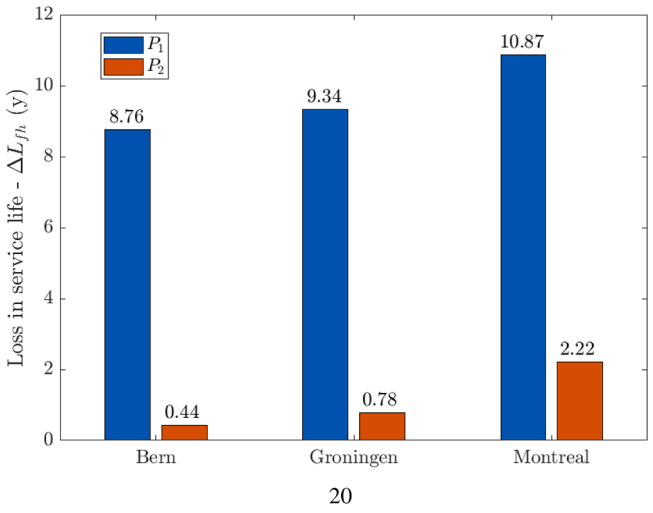

Fig. 7. Expected loss in service life years due to hail damage over a reference life of 25 years.

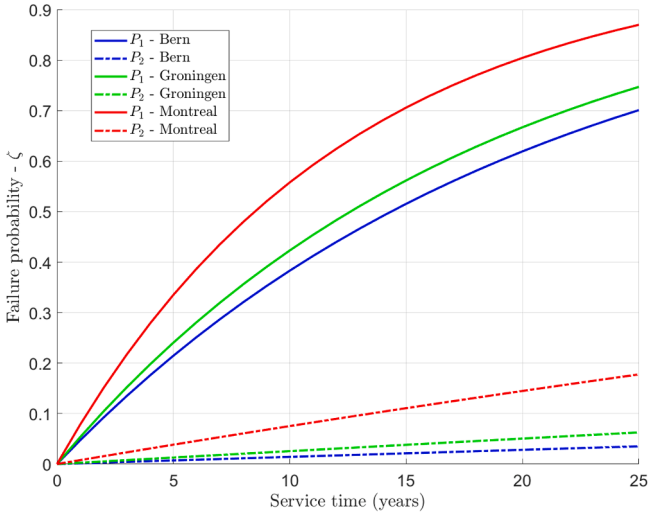

Fig. 8. Failure probability, ζ trend over the service life.

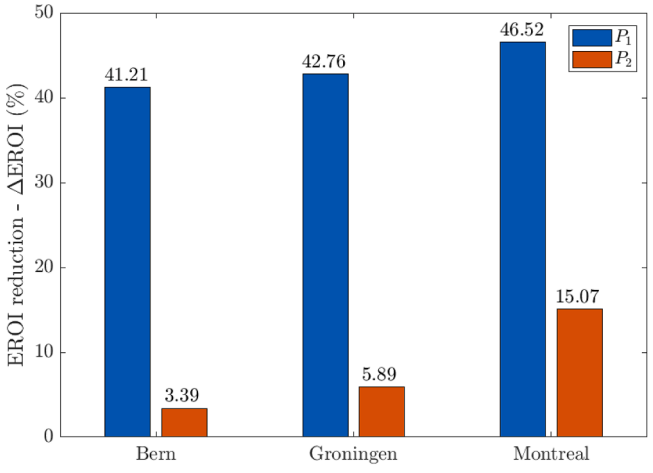

Fig. 9. Expected reduction of the EROI due to hail damage.

Table 3
Values of ratios Mr and Cr according to γ_{SFH} and γ_{AB}.

Location	Panel type	Mr (%)		Cr (%)	
		SFH	AB	SFH	AB
Bern	P_1	49	5	75	8
	P_2	1.5	0.1	2	0.2
Groningen	P_1	0.70	0.07	1.07	0.11
	P_2	0.03	0.003	0.05	0.005
Montreal	P_1	118	12	180	18
	P_2	12	1	18	2

in the case of Montreal. Conversely, the same consequence ratios are much lower for P_2 panels, being above 10% only in SHF in Montreal. It is worth recalling that the comparisons in Table 3 do not differentiate by specific building characteristics and thus constitute an expected average. A more precise assessment would require higher details in components definition, i.e. roofs, ETICS, windows etc, and their hail vulnerability.

4. Discussion

4.1. Practical implications

4.1.1. Standards and building codes

M_{pv}, C_{pv}, ΔLf_h and $\Delta EROI_h$, especially those calculated for P_1, appear significant. Still, P_1 panels were compliant with the international IEC 61,215 [28] and the compliance was also confirmed by the experimental tests of [25]. Hence, it may be argued that the minimum mandatory hailstone size, and consequently, the terminal velocity, for the IEC 61,215 should be increased. It is also evident that risk metrics for P_2 panels show a 4-5 fold variation on average across the different locations. This underlines that risk metrics are highly site-specific and depend significantly on hazard levels. Hence, another option could be shifting from optional to mandatory tests at higher hailstone sizes and velocities with resulting class-based minimum resistances. The relevant PV resistance classes will then be selected by designers or set as minimum performance by authorities following the site-specific hazard level. In this respect, countries like Switzerland [27] have already implemented independent testing protocols more stringent than the IEC 6125. Similarly, some manufacturers offer products with higher resistance. Finally, it has to be considered that in some countries, for instance Italy with the NTC 2018 [89], building codes have started including integrity and serviceability provisions on technical components. As more and more components will be placed on the exterior of the building envelope, such as BMPV or external heat pump compressors, other codes and standards will require additional checks on technical systems, as is the case for classic structural and non-structural components.

4.1.2. Mitigation measures

An increase of Tg, from 3.2 mm in P_1 panels to 4 mm in P_2 panels, can significantly reduce hail risk. For instance, ΔLf_h vary from 8.76-10.87 years range for P_1 to 0.44-2.22 years for P_2. At the same time, the variation in the P_2 range is not negligible as already underlined. These two considerations suggest that even higher Tg may be effective to protect PV panels in locations characterized by higher hazard levels. Nonetheless, other possible mitigation measures may be considered, such as active systems deploying shields on PV or varying the inclination angles [90]. Although these solutions are already present in the market to a certain extent, the approach adopted in this work may provide a cost-benefit analysis.

4.1.3. Building components fragility

The results confirm previous research that underlined the importance of hail risk for several building components [37,38]. Indeed, given

the comparison values from Table 3, hail damage to BMPV may represent up to 118% of a building total damages. Hence, it is reasonable to think that a component-based approach to hail risk assessment for buildings may prove an effective strategy. At the same time, this approach relies more on bottom-up assessment rather than higher details in empirical post-disaster analyses such as [32,73]. A component-based approach may also be useful in the case of BIPV [91] where vulnerable components could represent a non-negligible share of the building envelope. Furthermore, probabilistic risk assessment could be also extended to other external components such as heat pumps [92] and ETICS [35] where current testing requirements are either absent or possibly not demanding enough. In general, whilst the component-based approach is critical in building risk assessment [47,93], it is still rather unused in the case of integration with life cycle analysis [94].

4.1.4. Replicability of the methodology

The methodology presented in Section 2 can effectively be applied in other contexts to assess the impact of hail hazard on the life cycle of PV panels. The inputs required are a hazard and a fragility model sharing the same IM as in our case, Dh. Moreover, the definition of consequence metrics, such as unit cost and emissions, allows the estimation of EALs. It is, however, important to consider that such metrics should be normalised on As, since the area of the system under study affects the hazard level. This aligns with risk assessment for other components such as roofs [38] and cladding panels [37], where the area has been accounted for.

4.2. Limitations

Starting from the hazard models used in Section 2.1, the approach and data adopted have two main limitations. First, data on the return time of 100 years, which was the highest available for Switzerland and the Netherlands models is not sufficient. For reference, a 0.1% EAL, which is quite significant for risk assessment of buildings [6], is the result of a theoretical $1 \cdot 10^{-3}$ annual rate combined with an expected damage of 100%. Although a linear interpolation in a semi-log space can be a solution, it may carry a certain degree of approximation. Second, the conversion from MESHE area to A_s was performed for all the locations according to the analytical solution of the Swiss model [65]. A site-specific conversion law would probably improve the accuracy of the results.

Passing to the BMPV response model presented in Section 2.2.1, it has to be considered that available experimental data on front glass response at higher hailstone sizes and for different thicknesses are rather scarce. Hence, the fragility functions of Fig. 4 have been derived with a few assumptions based on the experimental results from [25]. For the sake of discussion, varying the lower and higher probability bounds from 0.05 and 0.95 to 0.20 and 0.80 would have resulted in a variation of the EROI reduction in the order of 1% max. This underscores that the risk metrics results are not so influenced by the fragility curve parameter β. Nonenetheless, in this respect, more tests on covering more and higher hailstone sizes would be needed. Along the same line, in this work, we have only considered a failure mode equivalent to a very severe breakage. However, failure modes with less severe consequences may still influence the overall risk, as it is known for damage accumulation phenomena in glass material [21,72]. In this case, the hailstorm hit rate could integrate the hazard model [37,38]. This is similar to other natural hazards, such as earthquakes, where simulating the effects of the time history of external forces may prove superior to using a single value IM [95,96]. Accuracy limitations are, however, in line with the results of previous empirical studies [22,24], where the relationship between hail size and damage is affected by high uncertainty.

Concerning building response model in Section 2.2.2, the empirical data from [32] do not differentiate by building type, nor geometry, or other construction characteristics. Such characteristics, and, as discussed before, the presence of vulnerable components, may indeed influence the response model and consequently the risk levels. Finally, the consequence metrics used in Section 2.3 are derived from average values, selected to provide an estimate of the risk levels. Still, these metrics could vary based, for BMPV, on the specific products and, for buildings, on the characteristics of the construction and other site-specific factors. There could be correlations between Tg and UC, EC, Lf and the EROI, entailing possible offsets between resistance and any performance metrics. For instance, according to mechanical testing of [97], mono-crystalline and poly-crystalline have different resistance to impact. In this context, an accurate risk assessment should account for these effects.

5. Conclusion and future developments

This work has investigated the impact of hail hazard on the life cycle of BMPV systems. An analytical framework based on PBE methodology has been adopted for hail risk assessment. Hail hazard models from three geographical regions, corresponding to the areas of Bern, Groningen and Montreal, are employed to predict annual occurrence depending on maximum hailstone sizes. Experimental and empirical data are used to build response models of BMPVs with different front glass thicknesses and of whole buildings. The analyses relied on consequence metrics to estimate expected monetary cost, embodied carbon emission, loss of service life and EROI reduction of BMPVs.

The main conclusions, in relation to the goals presented in Section 1, are outlined below:

1) PBE-based approach is a viable methodology for hail risk assessment. In particular, maximum hailstone size can be used as the intensity measure for both hazard and response models. Hence, hailstone sizes should be described in terms of annual occurrence and induced damage upon impact on the system under study.
2) Expected annual costs and emissions, due to hail risk, are in the range of 16.5–27.42 €and 7.54-12.54 $kgCO_{2eq}$ per square meter of panels with front glass of up to 3.2 mm thickness. The range is 0.5 - 2.72 €and 0.23-1.25 $kgCO_{2eq}$ in case of a 4 mm thickness. The loss of service life amounts to 8.76-10.87 years and 0.44-2.22 years for 3.2 mm and 4 mm thicknesses, respectively. The expected EROI reduction is in the ranges of 41.21–46.52% and 3.39-15.07% for 3.2 mm and 4 mm thicknesses, respectively. It can be concluded that hail risk is significant and should not be neglected in life cycle analyses of BMPVs.
3) Monetary costs and emissions due to BMPVs can be comparable or even higher, up to 118% of costs and 180% of emissions, than the hail hazard impact on the whole building. This is especially true for single-family houses with low glass thicknesses BMPVs in areas characterized by higher hazard levels.

These results can support policymakers in improving minimum mandatory hail resistance for PV panels and, in general, for hail risk management of the building stock. Moreover, system designers may adopt the presented framework to assess the costs and benefits of panel characteristics and possible mitigation measures. Several limitations of the study have also been discussed. In particular, the definition and application of the proposed design method could be improved by future research along the following lines: i) definition of hail hazard models for more geographies, focusing on intensity measures adoptable in risk assessment frameworks; ii) experimental tests covering a wider range of hailstone sizes, panel characteristics, and inclination angle to produce better response models able to inform generalizable FEMs; iii) experimental investigation of damage accumulation effects; iv) study of the correlations between hail resistance and other panel performances metrics, including costs and emissions; v) evaluation of alternative mitigation measures for panels protection, vi) perform a

sensitivity analysis on the various parameters influencing the hail risk assessment.

CRediT authorship contribution statement

Rocco di Filippo: Writing – original draft, Software, Methodology, Investigation, Formal analysis, Data curation, Conceptualization; **Gianluca Maracchini:** Writing – review & editing, Validation, Supervision, Project administration, Funding acquisition; **Rosa Di Maggio:** Writing – review & editing, Validation, Supervision, Project administration, Funding acquisition; **Oreste S. Bursi:** Writing – review & editing, Validation, Supervision, Project administration, Funding acquisition; **Rossano Albatici:** Writing – review & editing, Validation, Supervision, Project administration, Funding acquisition.

Data availability

Data will be made available on request.

Declaration of competing interest

The authors declare that they have no known competing financial interests or personal relationships that could have appeared to influence the work reported in this paper.

Acknowledgment

This work has been funded by the University of Trento in the framework of the project BETTER (CUP E63C22000500003). The second, third and fourth authors acknowledge the Italian Ministry of Education, Universities, and Research (MUR) in the framework of the project DICAM-EXC (Departments of Excellence 2023–2027, grant L232/2016). The second author also acknowledges the National Project MUR PNRR M4C2-CN1-SPOKE 9.

References

[1] UN, United Nations Environment Programme (2021), Global Status Report for Buildings and Construction: Towards a Zero-emission, Efficient and Resilient Buildings and Construction Sector, Technical Report, Nairobi, Kenya, 2021. https://globalabc.org/resources/publications/2021-global-status-report-buildings-and-construction.

[2] UN, United Nations, Mapping of Existing Energy Efficiency Standards and Technologies in Buildings in the UNECE Region, ECONOMIC COMMISSION FOR EUROPE Joint Task Force on Energy Efficiency Standards in Buildings, United Nations, Geneve, 2018. https://unece.org/info/publications/pub/2917.

[3] H. Zhang, K. Hewage, H. Karunathilake, H. Feng, R. Sadiq, Research on policy strategies for implementing energy retrofits in the residential buildings, J. Build. Eng. 43 (2021) 103161. https://doi.org/10.1016/j.jobe.2021.103161

[4] K. Amasyali, N.M. El-Gohary, A review of data-driven building energy consumption prediction studies, Renew. Sustain. Energy Rev. 81 (2018) 1192–1205. https://doi.org/10.1016/j.rser.2017.04.095

[5] D. Pan, Y. Bai, M. Chang, X. Wang, W. Wang, The technical and economic potential of urban rooftop photovoltaic systems for power generation in Guangzhou, China, Energy Build. 277 (2022) 112591. https://doi.org/10.1016/j.enbuild.2022.112591

[6] R. di Filippo, G. Maracchini, A probabilistic framework for stranding risk assessment and EPBD IV scenario analysis for the Italian building stock, J. Build. Eng. 96 (2024) 110448. https://doi.org/10.1016/j.jobe.2024.110448

[7] E. Ohene, A.P.C. Chan, A. Darko, Review of global research advances towards net-zero emissions buildings, Energy Build. 266 (2022) 112142. https://doi.org/10.1016/j.enbuild.2022.112142

[8] M. Sodhi, L. Banaszek, C. Magee, M. Rivero-Hudec, Economic lifetimes of solar panels, Procedia CIRP 105 (2022) 782–787. The 29th CIRP Conference on Life Cycle Engineering, April 4, – 6, 2022, Leuven, Belgium., https://doi.org/10.1016/j.procir.2022.02.130

[9] W.S. Ebhota, P.Y. Tabakov, Integrating rooftop PV system in low-cost building plan: a pathway to improving energy access and environmental sustainability, Energy Build. 344 (2025) 116020. https://doi.org/10.1016/j.enbuild.2025.116020

[10] M. Libra, D. Mrázek, I. Tyukhov, L. Severová, V. Poulek, J. Mach, T. Šubrt, V. Beránek, R. Svoboda, J. Sedláček, Reduced real lifetime of PV panels – economic consequences, Sol. Energy 259 (2023) 229–234. https://doi.org/10.1016/j.solener.2023.04.063

[11] M. Aghaei, A. Fairbrother, A. Gok, S. Ahmad, S. Kazim, K. Lobato, G. Oreski, A. Reinders, J. Schmitz, M. Theelen, P. Yilmaz, J. Kettle, Review of degradation and failure phenomena in photovoltaic modules, Renew. Sustain. Energy Rev. 159 (2022) 112160. https://doi.org/10.1016/j.rser.2022.112160

[12] O. Alavi, I. Kaaya, R. De Jong, W. De Ceuninck, M. Daenen, Assessing the impact of PV panel climate-based degradation rates on inverter reliability in grid-connected solar energy systems, Heliyon 10 (3) (2024) e25839. https://doi.org/10.1016/j.heliyon.2024.e25839

[13] L. Papargyri, P. Papanastasiou, G.E. Georghiou, Effect of materials and design on PV cracking under mechanical loading, Renew. Energy 199 (2022) 433–444. https://doi.org/10.1016/j.renene.2022.09.009

[14] O. Bamisile, C. Acen, D. Cai, Q. Huang, I. Staffell, The environmental factors affecting solar photovoltaic output, Renew. Sustain. Energy Rev. 208 (2025) 115073. https://doi.org/10.1016/j.rser.2024.115073

[15] L. Alfieri, P. Burek, L. Feyen, G. Forzieri, Global warming increases the frequency of river floods in Europe, Hydrol. Earth Syst. Sci. 19 (5) (2015) 2247–2260. https://doi.org/10.5194/hess-19-2247-2015

[16] R. Snaiki, S.S. Parida, Climate change effects on loss assessment and mitigation of residential buildings due to hurricane wind, J. Build. Eng. 69 (2023) 106256. https://doi.org/10.1016/j.jobe.2023.106256

[17] G. Forzieri, L. Feyen, S. Russo, M. Vousdoukas, L. Alfieri, S. Outten, M. Migliavacca, A. Bianchi, R. Rojas, A. Cid, Multi-hazard assessment in Europe under climate change, Clim. Change 137 (1-2) (2016) 105–119. https://doi.org/10.1007/s10584-016-1661-x

[18] S. Patel, L. Ceferino, C. Liu, A. Kiremidjian, R. Rajagopal, The disaster resilience value of shared rooftop solar systems in residential communities, Earthq. Spectra 37 (4) (2021) 2638–2661. https://doi.org/10.1177/87552930211020020

[19] L. Ceferino, N. Lin, Hurricane risk of solar generation in the United States, Nat. Hazards Rev. 24 (4) (2023) 04023029. https://doi.org/10.1061/NHREFO.NHENG-1764

[20] L. Ceferino, N. Lin, D. Xi, Bayesian updating of solar panel fragility curves and implications of higher panel strength for solar generation resilience, Reliab. Eng. Syst. Saf. 229 (2023) 108896. https://doi.org/10.1016/j.ress.2022.108896

[21] W. Muehleisen, G.C. Eder, Y. Voronko, M. Spielberger, H. Sonnleitner, K. Knoebl, R. Ebner, G. Ujvari, C. Hirschl, Outdoor detection and visualization of hailstorm damages of photovoltaic plants, Renew. Energy 118 (2018) 138–145. https://doi.org/10.1016/j.renene.2017.11.010

[22] T. Teule, M. Appeldoorn, P. Bosma, L. Sprenger, E. Koks, H. de Moel, The Vulnerability of Solar Panels to Hail, Technical Report, Vrije Universiteit Amsterdam, 2019. https://research.vu.nl/en/publications/the-vulnerability-of-solar-panels-to-hail.

[23] R.P. Vinay Gupta, Madhu Sharma, K.N.D. Babu, Impact of hailstorm on the performance of PV module: a review, Energy Sources A Recovery Util. Environ. Eff. 44 (1) (2022) 1923–1944. https://doi.org/10.1080/15567036.2019.1648597

[24] D.C. Jordan, K. Perry, R. White, C. Deline, Extreme weather and PV performance, IEEE J. Photovolt. 13 (6) (2023) 830–835. https://doi.org/10.1109/JPHOTOV.2023.3304357

[25] S. Chakraborty, A.K. Haldkar, N. Manoj Kumar, Analysis of the hail impacts on the performance of commercially available photovoltaic modules of varying front glass thickness, Renew. Energy 203 (2023) 345–356. https://doi.org/10.1016/j.renene.2022.12.061

[26] P. Bonomo, F. Parolini, P. Corti, F. Frontini, G. Bellenda, M. Caccivio, Impact resistance of BIPV systems: new testing procedure for performance assessment of multifunctional products, Energy Sci. Eng. 11 (1) (2023) 22–47. https://doi.org/10.1002/ese3.1364

[27] E. Cadoni, D. Forni, M. Dotta, G. Bellenda, M. Caccivio, Advanced characterisation of photovoltaics for hail resistance, Mater. Lett. 354 (2024) 135371. https://doi.org/10.1016/j.matlet.2023.135371

[28] International Electrotechnical Commission, Terrestrial Photovoltaic (PV) Modules - Design Qualification and Type Approval - Part 1: Test Requirements, Technical Report IEC 61215-1:2021, International Electrotechnical Commission, Geneva, Switzerland, 2021. https://webstore.iec.ch/en/publication/61345.

[29] International Electrotechnical Commission, IEC TS 63397:2022. Photovoltaic Modules – Extended Hail Test, Technical Report, International Electrotechnical Commission, 2022. Includes Corrigendum 1:2023, https://webstore.iec.ch/publication/68735.

[30] H.J. Punge, M. Kunz, Hail observations and hailstorm characteristics in Europe: a review, Atmos. Res. 176-177 (2016) 159–184. https://doi.org/10.1016/j.atmosres.2016.02.012

[31] M.H. Kim, J. Lee, S.-J. Lee, Hail: mechanisms, monitoring, forecasting, damages, financial compensation systems, and prevention, Atmosphere 14 (11) (2023). https://doi.org/10.3390/atmos14111642

[32] T. Schmid, R. Portmann, L. Villiger, K. Schröer, D.N. Bresch, An open-source radar-based hail damage model for buildings and cars, Nat. Hazards Earth Syst. Sci. 24 (3) (2024) 847–872. https://doi.org/10.5194/nhess-24-847-2024

[33] E. Elnagar, C. Düvier, Z. Batra, J. Christoffersen, C. Mandin, M. Schweiker, P. Wargocki, Creating a comprehensive framework for design, construction and management of healthy buildings, Energy Build. 324 (2024) 114883. https://doi.org/10.1016/j.enbuild.2024.114883

[34] S. Yeo, R. Leigh, I. Kuhnel, The April 1999 Sydney hailstorm, Aust. J. Emerg. Manag. 14 (1999) 23–25.

[35] B. Francke, R. Zamorowska, Resistance of external thermal insulation composite systems with rendering (ETICS) to hail, Materials 13 (11) (2020). https://doi.org/10.3390/ma13112452

[36] V. Steinbauer, J. Kaufmann, R. Zurbriggen, T. Bühler, M. Herwegh, Tracing hail stone impact on external thermal insulation composite systems (ETICS) – an evaluation of standard admission impact tests by means of high-speed-camera recordings, Int. J. Impact Eng. 109 (2017) 354–365. https://doi.org/10.1016/j.ijimpeng.2017.07.016

[37] S. Shi, N. Lam, Y. Cui, G. Lu, E. Gad, L. Zhang, Life-cycle performance of aluminium cladding panels in resisting hailstorms, Struct. Saf. 108 (2024) 102439. https://doi.org/10.1016/j.strusafe.2024.102439

[38] K. Porter, A benefit-cost analysis of impact-resistant asphalt shingle roofing, building resilient communities / Bâtir des communautés résilientes, Smart PROGRAM (March 2022), https://www.hail-smart.com/wp-content/uploads/2022/05/Benefit-cost-analysis-of-Impact-resistant-asphalt-shingle-roofing2.pdf.

[39] Y. Li, K. Porter, K. Goda, Hail hazard modeling with uncertainty analysis and roof damage estimation of residential buildings in North America, Int. J. Disaster Risk Reduct. 113 (2024) 104853. https://doi.org/10.1016/j.ijdrr.2024.104853

[40] C.A. Cornell, H. Krawinkler, Progress and challenges in seismic performance assessment, 2000, (PEER Center News). http://peer.berkeley.edu.

[41] N. Attary, V.U. Unnikrishnan, J.W. van de Lindt, D.T. Cox, A.R. Barbosa, Performance-based tsunami engineering methodology for risk assessment of structures, Eng. Struct. 141 (2017) 676–686.

[42] M. Barbato, F. Petrini, V.U. Unnikrishnan, M. Ciampoli, Performance-based hurricane engineering (PBHE) framework, Struct. Saf. 45 (2013) 24–35.

[43] R. di Filippo, O.S. Bursi, R. di Maggio, Global warming and ozone depletion potentials caused by emissions from HFC and CFC banks due structural damage, Energy Build. 273 (2022) 112385. https://doi.org/10.1016/j.enbuild.2022.112385

[44] F. Jalayer, S. Carozza, R. De Risi, G. Manfredi, E. Mbuya, Performance-based flood safety-checking for non-engineered masonry structures, Eng. Struct. 106 (2016) 109–123. https://doi.org/10.1016/j.engstruct.2015.10.007

[45] R.A. Salgado, S. Guner, A structural performance-based environmental impact assessment framework for natural hazard loads, J. Build. Eng. 43 (2021) 102908. https://doi.org/10.1016/j.jobe.2021.102908

[46] D. Lange, S. Devaney, A. Usmani, An application of the PEER performance based earthquake engineering framework to structures in fire, Eng. Struct. 66 (2014) 100–115.

[47] R. di Filippo, L. Possidente, N. Tondini, O.S. Bursi, Quantitative integration of probabilistic fire risk assessment with LCA of buildings: the environmental impact of thermal insulation design, J. Build. Eng. 160 (2023) 683–694. https://doi.org/10.1016/j.psep.2022.02.042

[48] R. di Filippo, O.S. Bursi, M. Ragazzi, M. Ciucci, Natech risk and the impact of high-GWP content release on LCA of industrial components, Process Saf. Environ. Prot. 160 (2022) 683–694. https://doi.org/10.1016/j.psep.2022.02.042

[49] G. Maracchini, R. di Filippo, R. Albatici, O.S. Bursi, R. Di Maggio, Sustainable retrofit of existing buildings: impact assessment of residual fluorocarbons through uncertainty and sensitivity analyses, Energies 16 (7) (2023). https://doi.org/10.3390/en16073276

[50] R. di Filippo, G. Maracchini, R. Albatici, R. Di Maggio, O.S. Bursi, A novel prescriptive approach for buildings' insulation design considering embodied carbon, Renew. Sustain. Energy Rev. 212 (2025) 115369. https://doi.org/10.1016/j.rser.2025.115369

[51] H.M. Wikoff, S.B. Reese, M.O. Reese, Embodied energy and carbon from the manufacture of cadmium telluride and silicon photovoltaics, Joule 6 (7) (2022) 1710–1725. https://doi.org/10.1016/j.joule.2022.06.006

[52] A. Galimshina, J. McCarty, C. Waibel, A. Schlueter, A. Hollberg, High-resolution parametric embodied impact configurator for PV and BIPV systems, Renew. Energy 236 (2024) 121404. https://doi.org/10.1016/j.renene.2024.121404

[53] M.R. Sers, P.A. Victor, The energy-emissions trap, Ecol. Econ. 151 (2018) 10–21. https://doi.org/10.1016/j.ecolecon.2018.04.004

[54] B. Al Shawa, Should we stop installing vertical photovoltaics on building façades?, Energy Build. 344 (2025) 115978. https://doi.org/10.1016/j.enbuild.2025.115978

[55] F. Ferroni, R.J. Hopkirk, Energy return on energy invested (ERoEI) for photovoltaic solar systems in regions of moderate insolation, Energy Policy 94 (2016) 336–344. https://doi.org/10.1016/j.enpol.2016.03.034

[56] M. Raugei, S. Sgouridis, D. Murphy, V. Fthenakis, R. Frischknecht, C. Breyer, U. Bardi, C. Barnhart, A. Buckley, M. Carbajales-Dale, D. Csala, M. de Wild-Scholten, G. Heath, A. Jæger-Waldau, C. Jones, A. Keller, E. Leccisi, P. Mancarella, N. Pearsall, A. Siegel, W. Sinke, P. Stolz, Energy return on energy invested (ERoEI) for photovoltaic solar systems in regions of moderate insolation: a comprehensive response, Energy Policy 102 (2017) 377–384. https://doi.org/10.1016/j.enpol.2016.12.042

[57] J.W. Baker, Efficient analytical fragility function fitting using dynamic structural analysis, Earthq. Spectra 31 (1) (2015) 579–599. http://journals.sagepub.com/doi/10.1193/021113EQS025M. https://doi.org/10.1193/021113EQS025M

[58] D. Meng, S. Yang, A.M.P. de Jesus, S.-P. Zhu, A novel Kriging-model-assisted reliability-based multidisciplinary design optimization strategy and its application in the offshore wind turbine tower, Renew. Energy 203 (2023) 407–420. https://doi.org/10.1016/j.renene.2022.12.062

[59] S. Yang, D. Meng, H. Yang, B. Keshtegar, A.M.P. De Jesus, S.-P. Zhu, Adaptive Kriging-assisted enhanced sparrow search with augmented-Lagrangian first-order reliability method for highly efficient structural reliability analysis, Reliab. Eng. Syst. Saf. 267 (2026) 111916. https://doi.org/10.1016/j.ress.2025.111916

[60] S. Yang, D. Meng, M. Alfouneh, B. Keshtegar, S.-P. Zhu, A robust-weighted hybrid nonlinear regression for reliability based topology optimization with multi-source uncertainties, Comput. Methods Appl. Mech. Eng. 447 (2025) 118360. https://doi.org/10.1016/j.cma.2025.118360

[61] J. Grieser, M. Hill, How to express hail intensity—modeling the hailstone size distribution, J. Appl. Meteorol. Climatol. 58 (10) (2019) 2329–2345. https://doi.org/10.1175/JAMC-D-18-0334.1

[62] D. Forni, M. Caccivio, D. Chudy, E. Cadoni, An experimental investigation of ice ball impact behaviour to improve PV panel hailstone safety, Int. J. Impact Eng. 202 (2025) 105315. https://doi.org/10.1016/j.ijimpeng.2025.105315

[63] L. Wouters, M. Boon, D. van Putten, B. van 't Veen, E. Koks, H. de Moel, A Hail Climatology of the Netherlands, Technical Report, IVM Institute for Environmental Studies, Vrije Universiteit Amsterdam, 2019. Accessed: 2025-03-04, https://research.vu.nl/en/publications/6ff0b1d2-863b-42f6-9f13-b88127569027.

[64] K. Schröer, S. Trefalt, A. Hering, U. Germann, C. Schwierz, Hagelklima Schweiz: Daten, Ergebnisse und Dokumentation, Technical Report 283, Fachbericht MeteoSchweiz, 2022. https://doi.org/10.18751/PMCH/TR/283.HagelklimaSchweiz/1.0

[65] U. Germann, M. Boscacci, L. Clementi, M. Gabella, A. Hering, M. Sartori, I.V. Sideris, B. Calpini, Weather radar in complex orography, Remote Sens. 14 (3) (2022). https://doi.org/10.3390/rs14030503

[66] D. Etkin, Hail climatology for canada: an update, 2018, Accessed: 2025-03-04, https://www.iclr.org/wp-content/uploads/2018/03/hail-climatology-for-canada-an-update.pdf.

[67] I. Iervolino, Assessing uncertainty in estimation of seismic response for PBEE, Earthq. Eng. Struct. Dyn. 46 (13) (2017) 1711–1723. https://doi.org/10.1002/eqe.2883

[68] F. De Martin, A. Manzato, N. Carlon, S. Carpentari, F. Pavan, G. Cioni, M.M. Miglietta, European record-breaking hailstorms in Northern Italy on 19 and 24 July 2023, in: 4th European Hail Workshop, 2024. Accessed: 2025-05-20, https://cris.unibo.it/handle/11585/999148?mode=simple.

[69] S. Matalucci, Chicchi di grandine di almeno 3 cm: maggiore problema per pannelli solari, studio VUA, 2023, Accesso: 2025-05-20, https://www.pv-magazine.it/2023/07/26/chicchi-di-grandine-di-almeno-3-cm-maggiore-problema-per-pannelli-solari-studio-vua/.

[70] C. Dieling, M. Smith, M. Beruvides, Review of impact factors of the velocity of large hailstones for laboratory hail impact testing consideration, Geosciences 10 (12) (2020). https://doi.org/10.3390/geosciences10120500

[71] U. S. Department of Energy, Hail damage mitigation for solar photovoltaic systems, 2024, Accessed: 2025-05-19, https://www.energy.gov/femp/hail-damage-mitigation-solar-photovoltaic-systems.

[72] Y. Cui, N. Lam, S. Shi, E. Gad, L. Zhang, Fragility curves for hail resistance of toughened glass, J. Build. Eng. 104 (2025) 112249. https://doi.org/10.1016/j.jobe.2025.112249

[73] L. Ackermann, J. Soderholm, A. Protat, R. Whitley, L. Ye, N. Ridder, Radar and environment-based hail damage estimates using machine learning, Atmos. Meas. Tech. 17 (2) (2024) 407–422. https://doi.org/10.5194/amt-17-407-2024

[74] M. Dolce, A. Prota, B. Borzi, F. da Porto, S. Lagomarsino, G. Magenes, C. Moroni, A. Penna, M. Polese, E. Speranza, G. M. Verderame, G. Zuccaro, Seismic risk assessment of residential buildings in Italy, Bull. Earthq. Eng. (2021). https://doi.org/10.1007/s10518-020-01009-5

[75] G. Tocchi, D. Ottonelli, N. Rebora, M. Polese, Multi-risk assessment in the veneto region: an approach to rank seismic and flood risk, Sustainability 15 (16) (2023). https://doi.org/10.3390/su151612458

[76] UBS Insights, Building a house: important facts and tips, 2024, Accessed: 2025-04-15, https://www.ubs.com/ch/en/services/guide/mortgages-and-financing/articles/tips-for-building-a-house.html.

[77] Neho, Real estate m^2 price in Switzerland in 2025, 2025, Accessed: 2025-04-15, https://neho.ch/en/real-estate-price-m2-switzerland.

[78] K. Emanuel, Global warming effects on U.S. hurricane damage, Weather Clim. Soc. 3 (4) (2011) 261–268. https://doi.org/10.1175/WCAS-D-11-00007.1

[79] H. Gholami, H.N. Røstvik, D. Müller-Eie, Holistic economic analysis of building integrated photovoltaics (BIPV) system: case studies evaluation, Energy Build. 203 (2019) 109461. https://doi.org/10.1016/j.enbuild.2019.109461

[80] F. Ascione, R.F. De Masi, M. Mastellone, S. Ruggiero, G.P. Vanoli, Improving the building stock sustainability in European countries: a focus on the Italian case, J. Clean. Prod. 365 (2022) 132699. https://doi.org/10.1016/j.jclepro.2022.132699

[81] V. Tirupati Rao, Y. Raja Sekhar, Comparative analysis on embodied energy and CO2 emissions for stand-alone crystalline silicon photovoltaic thermal (PVT) systems for tropical climatic regions of India, Sustain. Cities Soc. 78 (2022) 103650. https://doi.org/10.1016/j.scs.2021.103650

[82] M. Milousi, M. Souliotis, G. Arampatzis, S. Papaefthimiou, Evaluating the environmental performance of solar energy systems through a combined life cycle assessment and cost analysis, Sustainability 11 (9) (2019). https://doi.org/10.3390/su11092539

[83] D. Yang, J. Liu, J. Yang, N. Ding, Life-cycle assessment of China's multi-crystalline silicon photovoltaic modules considering international trade, J. Clean. Prod. 94 (2015) 35–45. https://doi.org/10.1016/j.jclepro.2015.02.003

[84] F. Ferroni, A. Guekos, R.J. Hopkirk, et al., Further considerations to: energy return on energy invested (ERoEI) for photovoltaic solar systems in regions of moderate insolation, Energy Policy 107 (2017) 498–505. https://doi.org/10.1016/j.enpol.2017.05.007

[85] E. Cutore, R. Volpe, R. Sgroi, A. Fichera, Energy management and sustainability assessment of renewable energy communities: the Italian context, Energy Convers. Manag. 278 (2023) 116713. https://doi.org/10.1016/j.enconman.2023.116713

[86] T. Huld, R. Müller, A. Gambardella, A new solar radiation database for estimating PV performance in Europe and Africa, Sol. Energy 86 (6) (2012) 1803–1815. https://doi.org/10.1016/j.solener.2012.03.006

[87] R. Lyons, G. O'Sullivan, B. Griffiths, E. McAuley, A. Bermingham, T. Gillespie, M. Guennewig-Moenert, L. Hauser, C.R. Diez, S. Shaikh, Building Homes: Apartment Construction Costs in Europe with a Focus on Dublin, Technical Report, Trinity College Dublin and Society of Chartered Surveyors Ireland, 2024. Accessed: 2025-04-23, https://scsi.ie/wp-content/uploads/2024/07/SCSI-TCD-Building-Homes-Report.pdf.

[88] M. Röck, A. Sørensen, B. Tozan, J. Steinmann, L.H. Horup, X.L. Den, H. Birgisdottir, Towards Embodied Carbon Benchmarks for Buildings in Europe: #2 Setting the Baseline – A Bottom-Up Approach, Technical Report, Rambøll and Aalborg University, 2022. Accessed: 2025-04-23, https://doi.org/10.5281/zenodo.5895051

[89] Ministero delle Infrastrutture e dei Trasporti, Aggiornamento delle Norme Tecniche per le Costruzioni, D.M. 17 gennaio 2018, Gazzetta Ufficiale della Repubblica Italiana n. 42 del 20-02-2018 - Suppl. Ordinario n. 8, Roma, Italia, 2018. Accessed: 2024-05-22, https://www.gazzettaufficiale.it/eli/id/2018/2/20/18A00716/sg.

[90] J. Previtali, Actionable insights to safeguard solar projects from hail damage, PV magazine USA, 2025. Accessed: 2025-05-19, https://pv-magazine-usa.com/2025/01/22/actionable-insights-to-safeguard-solar-projects-from-hail-damage/.

[91] H. Gholami, H.N. Røstvik, Economic analysis of BIPV systems as a building envelope material for building skins in Europe, Energy 204 (2020) 117931. https://doi.org/10.1016/j.energy.2020.117931

[92] Hail Effects on Air-Conditioner Performance, Volume 6: Energy Systems: Analysis, Thermodynamics and Sustainability of ASME International Mechanical Engineering Congress and Exposition, 2007. https://doi.org/10.1115/IMECE2007-41518

[93] R. di Filippo, G. Maracchini, D. Colbourne, R. Di Maggio, O.S. Bursi, Low-GWP flammable refrigerants and fire risk: the importance of leakage-induced vs reaction-influenced scenarios, Int. J. Disaster Risk Reduct. 122 (2025) 105453. https://doi.org/10.1016/j.ijdrr.2025.105453

[94] X. Tanguay, B. Amor, Assessing the sustainability of a resilient built environment: research challenges and opportunities, J. Clean. Prod. 458 (2024) 142437. https://doi.org/10.1016/j.jclepro.2024.142437

[95] O. Sayginer, R. di Filippo, A. Lecoq, et al., Seismic vulnerability analysis of a coupled tank-piping system by means of hybrid simulation and acoustic emission, Exp. Tech. 44 (2020) 807–819. https://doi.org/10.1007/s40799-020-00396-3

[96] G. Abbiati, M. Broccardo, R. di Filippo, B. Stojadinović, O.S. Bursi, Seismic fragility analysis of a coupled tank-piping system based on artificial ground motions and surrogate modeling, J. Loss Prev. Process Ind. 72 (2021) 104575. https://doi.org/10.1016/j.jlp.2021.104575

[97] H.B. Ali, M.A. Kamran, R.M. Gul, M. Yasir, F.T. Alabdullah, C. Usman, A. Tariq, Mechanical integrity of photovoltaic panels under hailstorms: mono vs. poly-crystalline comparison, Heliyon 10 (4) (2024) e25865. https://doi.org/10.1016/j.heliyon.2024.e25865